Lithos 380–381 (2021) 105824

Contents lists available at ScienceDirect

Lithos

journal homepage: www.elsevier.com/locate/lithos

Research Article

Fluid inclusion and stable isotope constraints on the source and evolution of ore-forming fluids in the Bailongshan pegmatitic Li-Rb deposit, Xinjiang, western China

Zeyang Zhang [a,b], Yuhang Jiang [a,*], Hecai Niu [a], Pan Qu [a,b]

[a] CAS Key Laboratory of Mineralogy and Metallogeny, Guangdong Provincial Key Laboratory of Mineral Physics and Materials, Guangzhou Institute of Geochemistry, Chinese Academy of Sciences, Guangzhou 510640, China
[b] University of Chinese Academy of Sciences, Beijing 100049, China

ARTICLE INFO

Article history:
Received 31 May 2019
Received in revised form 27 August 2020
Accepted 5 October 2020
Available online 8 October 2020

Keywords:
Bailongshan pegmatitic Li–Rb deposit
Fluid boiling
Supercritical fluid
CO_2-rich inclusions
H–O isotopes

ABSTRACT

The newly discovered Bailongshan pegmatitic lithium–rubidium (Li–Rb) deposit in West Kunlun–Karakorum (western China) is a world-class Li deposit. In this paper, we present detailed field observations and fluid inclusion (FI) data for four major mineral zones at Bailongshan; i.e., the fine albite (FAZ), blocky feldspar (BFZ), quartz–muscovite (QMZ), and spodumene–quartz (SQZ) zones. FIs are abundant in quartz and spodumene, and include four types: (1) two-phase L-type, (2) two-phase V-type, (3) three-phase S-type, and (4) three-phase (CO_2–H_2O–NaCl) or two-phase (CO_2-rich) C-type. Quartz contains all four FI types, whereas spodumene contains mainly C-type FIs. Microthermometric measurements show that the L-type FIs in the FAZ, BFZ, and SQZ homogenised at 283–338, 156–224, and 223–421 °C, respectively, with corresponding salinities of 15.4–26.5, 4.4–10.4, and 10.5–30.6 wt% NaCl equivalent. The S-type FIs in the FAZ and SQZ homogenised at 183–285 and 214–298 °C, respectively. The C-type FIs in spodumene and quartz homogenised at 256–321 and 234–286 °C, with corresponding salinities of 4.4–18.1 and 4.4–12.6 wt% NaCl equivalent, respectively. The ore-forming fluids were of medium–low-temperature and medium–low-salinity, and no systematic fluid compositional variations were identified in each zone. The average CO_2 densities and trapping pressures were estimated at 0.72–0.91 g/cm^3 and 3.00–3.75 kb, respectively, corresponding to mineralisation depths of 9–11 km. Supercritical fluids likely contributed to the concentration of ore-forming elements in the fluids, and fluid boiling may have led to CO_2 degassing and Li ore deposition. H–O isotope data show that quartz grains from all four zones have $\delta^{18}O_{V\text{-}SMOW}$ values of 8.6‰–10.2‰ and $\delta D_{V\text{-}SMOW}$ values of −38‰ to 107‰. The ore-forming fluids were likely sourced from pegmatitic magmas.

1. Introduction

Lithium is an important metal for new energy technologies and is in rapidly growing demand. Lithium-bearing pegmatites formed mainly in the Precambrian account for 26% of global Li resources e.g., Bessemer City, USA; Greenbushes, Australia; Bikita, Zimbabwe (Kesler et al., 2012; Liu et al., 2017). Studies of pegmatite-related rare-metal deposits have focused mainly on the formation of the pegmatites and mineral zoning, mineralisation mechanisms, and fluid evolution (London, 1986; Redden and Norton, 1990; Stewart, 1978). Granitic pegmatites usually contain a large amount of multiphase fluid inclusions (FIs), such as in the Tanco Li–Be deposit (Manitoba, Canada), Corin Li deposit (Sichuan, China), and No. 3 Ketouhai pegmatite vein (Xinjiang, China; Anderson et al., 2001; Landsman, 1984; London, 1986, 2018; Zhu et al., 2000). FIs can provide useful information on the physicochemical conditions of magma crystallisation and fluid evolution during pegmatite formation (Nabelek and Gammel, 2016; Smirnov, 2015; Thomas et al., 2009). However, FI studies of pegmatitic deposits are rare, and most studied FIs represent only the late-stage hydrothermal fluids because most pegmatites contain only secondary inclusions (Abella et al., 1995; Frezzotti et al., 1994; Fuertes-Fuente et al., 2000a; London, 1986, 1990; Smerekanicz and Francis, 1999; Trumbull, 1995). Based on data for the Tanco pegmatite, Černý (1991) and Ghavidel-syooki et al. (2015) suggested that Li–Cs–Ta (LCT)-type pegmatitic magmatic fluids have a high vapour phase content, low CO_2 content, low salinity, and undergo unmixing of the primary fluids into aqueous and carbonic components at subsolidus conditions. Ore-forming fluids in the Jiajika pegmatite deposit originated from differentiation of deep-seated granitic magmas (Li et al., 2006a, 2006b). London (1987) proposed that

* Corresponding author at: CAS Key Laboratory of Mineralogy and Metallogeny, Guangzhou Institute of Geochemistry, Chinese Academy of Sciences, Guangzhou 510640, China.
E-mail address: jiangyuhang@gig.ac.cn (Y. Jiang).

https://doi.org/10.1016/j.lithos.2020.105824
0024-4937/

hydrothermal metasomatism during the late differentiation of granitic pegmatites is closely related to rare-metal mineralisation. Nabelek et al. (2010) and Bartels et al. (2013, 2015) showed that dissolved H_2O has a key role in pegmatite formation by lowering the viscosity, reducing the glass transition temperature, and raising the free energy required for nucleation. Thomas and Williams (2018) revised the model for the regional zonation of the Lacorne rare-metal pegmatites, and suggested that higher volatile contents (H_2O, F, and Li) led to a progressively lower magma viscosity and rapid solidification. London et al. (1989) proposed that pegmatite crystallisation is a rapid, disequilibrium, and stepwise process. Fuertes-Fuente et al. (2000b) showed that the trapping conditions of FIs did not vary from the wall zone to the core of a pegmatite in the Black Hills, USA. Ackerman et al. (2007) investigated the fluid evolution and *P–T* conditions of Li-bearing and barren pegmatites in the same area, and found that the formation pressure of the Li-bearing pegmatites was lower than that of the barren pegmatite.

With Li_2O reserves of 3.45 million tonnes (Mt), the Bailongshan pegmatitic Li–Rb deposit is likely of giant scale. The deposit is located in the West Kunlun–Karakorum region of western China (Wang et al., 2017). Four mineral zones can be recognised in the deposit; i.e., the fine albite (FAZ), blocky feldspar (BFZ), quartz–muscovite (QMZ), and spodumene–quartz (SQZ) zones. Abundant primary FIs occur in the quartz and spodumene from these four zones in the Bailongshan deposit, which may provide insights into the source and evolution of the pegmatitic ore-forming fluids.

In this study, 18 representative rocks from the 4 mineral zones in the Bailongshan deposit were sampled. Systematic rock and FI petrographic observations, FI microthermometric and laser Raman spectroscopic analyses, and H–O stable isotope analyses were undertaken. These data were then used to investigate the fluid sources and evolution in the four distinct mineral zones and processes of Li mineralisation in the Bailongshan deposit.

2. Regional and ore deposit geology

The West Kunlun–Karakoram Orogen is located on the northwestern margin of the Tibetan Plateau, and consists of the North Kunlun, South Kunlun, Tianshuihai, and Karakoram terranes (Xu et al., 2018). Previous studies have suggested that the West Kunlun–Karakorum Orogen formed during the closure of the Proto-Tethys and Palaeo-Tethys oceans (Mattern et al., 1996; Xiao and Fan, 2001). The Bailongshan deposit is located in the eastern Tianshuihai terrane, between the Mazha–Kangxiwa and Qiaoer Tianshan–Hongshan Lake suture zones to its south and north, respectively (Fig. 1; Wang et al., 2017). Mesozoic granitic pegmatites are well-developed in this area, and host numerous Li–Be (Nb–Ta)-bearing rare-metal deposits, including the Bailongshan and nearby Dahongliutan deposits (Yan et al., 2016; Zhou et al., 2011). Three ore bodies have been identified at Bailongshan, which contain 3.45 Mt. Li_2O (at 1.26–1.60 wt%) and 170 kt Rb_2O.

This newly discovered superlarge deposit is located at over 4900 m above sea level, with a maximum altitude of 5800 m. The stratigraphy of the Bailongshan deposit is relatively simple and comprises mainly medium–high-grade metamorphic rocks of the Triassic Bayan–Kelashan Mountain Group and Quaternary glacial sediments (Fig. 1). The major rock types include greenschist-facies rocks, grey–green metasandstones, and two-mica quartz schists. Regional metamorphism (greenschist-facies) has widely affected the rocks in the mining area. The metamorphic mineral assemblage is quartz–plagioclase–muscovite–biotite–andalusite. The spodumene-bearing pegmatite veins in the Bailongshan deposit have intruded metasandstones. The major structures comprise predominantly WNW–ESE-trending faults. Fine-grained granodiorite has been widely emplaced in the southern Bailongshan deposit, and fine-grained muscovite granite intruded the northwestern part of the deposit. A total of 3750 m of WNW–ESE-trending, spodumene-bearing pegmatite dykes/lenses with widths of 46–165 m have been documented in the mining area, many of which reach ore grade (Wang et al., 2017).

Among these spodumene-bearing pegmatites, three large-scale ore bodies (1, 2, and 3) have been identified, and >10 smaller Li ore bodies have also been discovered. The No. 1 ore body is located in the western part of the mining area and strikes WNW–ESE. The surface of the mineralised body is ~1230 m long, 46–77 m wide, and 61.86 m thick (Fig. 2a). The No. 2 ore body is located in the central part of the mining area and strikes WNW–ESE. The surface of this mineralised body is ~1220 m long, 81–152 m wide, and 115.85 m thick. The No. 3 ore body is located in the eastern part of the mining area and also strikes WNW–ESE. The surface of this mineralised body is 990 m long, 60–152 m wide, and 97 m thick. The main ore mineral is spodumene, which is (light) grey in colour (Fig. 2b). Most of the ore minerals are thick platy crystals that interpenetrate between quartz and feldspar (Fig. 2c). The crystal size can be as large as 15–25 × 10 cm and exhibits a well-developed cleavage. The ores have banded and massive structures (Wang et al., 2017; Xu et al., 2018).

Local zoning is a common feature of pegmatites (London, 2005). Such zoning is thought to start from the ore-generating pluton, and forms by processes such as continuous/episodic melt extraction and fractional crystallisation along dyke margins (Černý, 1991; Trueman and Černý, 1982). In the Bailongshan deposit, there are four main zones (i.e., the FAZ, BFZ, QMZ, and SQZ).

The FAZ belongs to the border zone and consists of euhedral albite (50–75 vol%), K-feldspar (10–20 vol%), and mica (5–10 vol%; muscovite to lepidolite), along with minor apatite and tourmaline (Figs. 2d and 3a–c). White quartz aggregates are locally developed (Fig. 2d).

The BFZ belongs to the wall zone, and contains feldspar megacrysts (50–80 vol%), including mainly K-feldspar and minor albite and plagioclase (Figs. 2e and 3e). Quartz (15–30 vol%) occurs either as individual crystals or as aggregates in veins (Fig. 3d). Minor muscovite and tourmaline (<5 vol%) occur mainly in quartz veins.

The QMZ also belongs to the wall zone, and consists of quartz (40–60 vol%), albite (10–20 vol%), and muscovite (10–20 vol%; Figs. 2f and 3f). The quartz comprises early-stage coarse-grained and late-stage fine-grained vein types.

In the SQZ, the main ore mineral is pale grey, tabular spodumene intergrown with quartz and feldspar (Fig. 2b, g, and h). Rare spodumene grains are fine-grained and platy. The spodumene grain size is generally 10–30 × 2.5 mm, and the larger crystals are up to 15–25 × 10 cm in size (Fig. 2c; Wang et al., 2017). Quartz grains (20–35 vol%) can be divided into early-stage, milky white, medium–coarse-grained crystals (Q1), which are cut by late-stage, smoky grey, fine-grained vein quartz (Q2) that also cuts spodumene (Fig. 3h–k). The SQZ rocks also contain K-feldspar (10 to 25 vol%) and accessory apatite and columbite–tantalite (Fig. 3l).

3. Samples and methods

3.1. Sampling

A total of 50 samples were collected from the pegmatite dykes, and 52 polished thin-sections were prepared and examined using both transmitted and reflected light microscopy. Forty doubly polished thick-sections of quartz from the four mineral zones, and spodumene from the SQZ, were prepared for FI investigation, among which 20 were chosen for microthermometric measurements.

3.2. Microthermometry

We selected spodumene from the SQZ and quartz from all four zones for microthermometric analysis. In order to study the fluid evolution in different zones and stages, we analysed mainly primary inclusions, but also a small number of secondary inclusions; however, the FIs in the QMZ were too small to analyse. We estimate the salinities of the fluids

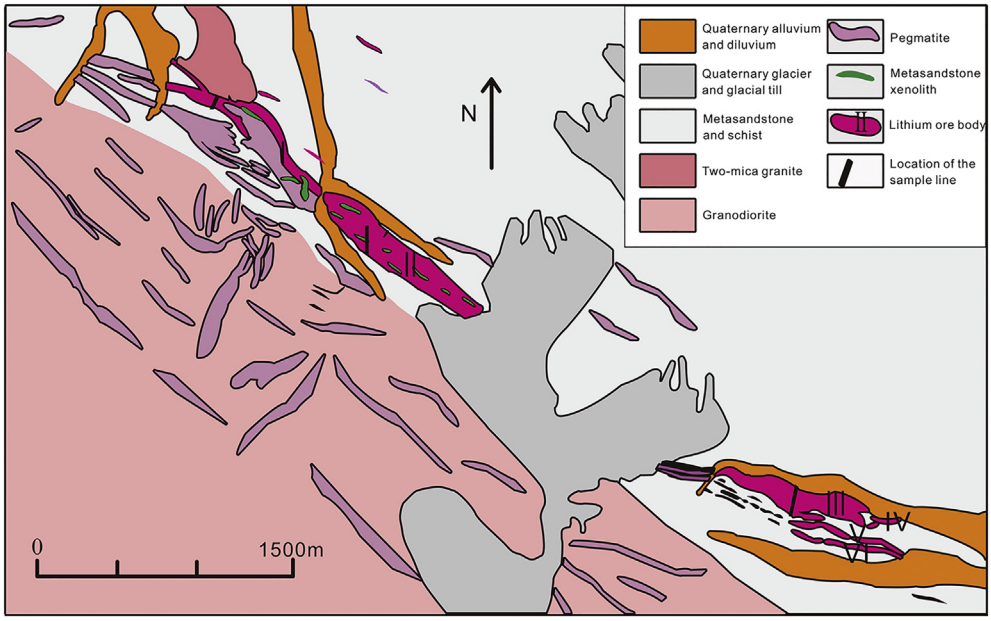

Fig. 1. Geological map of the major ore bodies in the Bailongshan pegmatite deposit, Karakorum (modified after Wang et al., 2017).

based on the freezing and melting temperatures of the L-type FIs, halite crystal melting temperatures of S-type FIs, and clathrate-compound disappearance temperature of C-type FIs.

The microthermometric measurements were carried out with a Linkam MDS 600 heating–freezing system at the Key Laboratory of Mineralogy and Metallogeny, Chinese Academy of Sciences, Guangzhou,

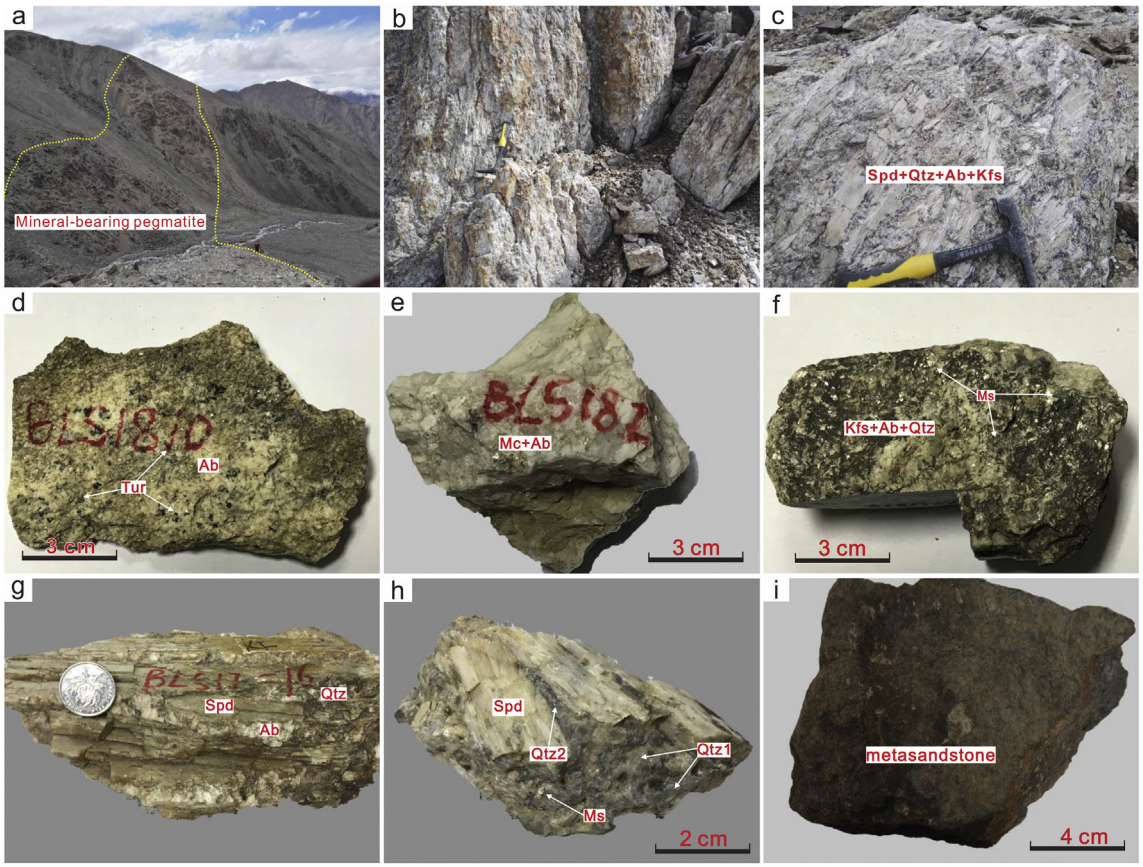

Fig. 2. Field and hand specimen photographs of the Bailongshan Li–Rb deposit. (a) The No. 1 pegmatite ore body. (b) Ore-bearing pegmatite. (c) Spodumene-rich pegmatite. (d) Hand specimen of the FAZ. (e) Hand specimen of the BFZ. (f) Hand specimen of the QMZ. (g) Columnar megacrysts. (h) Hand specimen of the SQZ. (i) Metasandstone wall-rock (Bayan Hara Group) of the Bailongshan pegmatite deposit. Abbreviations: Spd = spodumene; Qtz = quartz; Ab = albite; Kfs = K-feldspar; Ms. = muscovite; Mc = microcline; Tur = tourmaline.

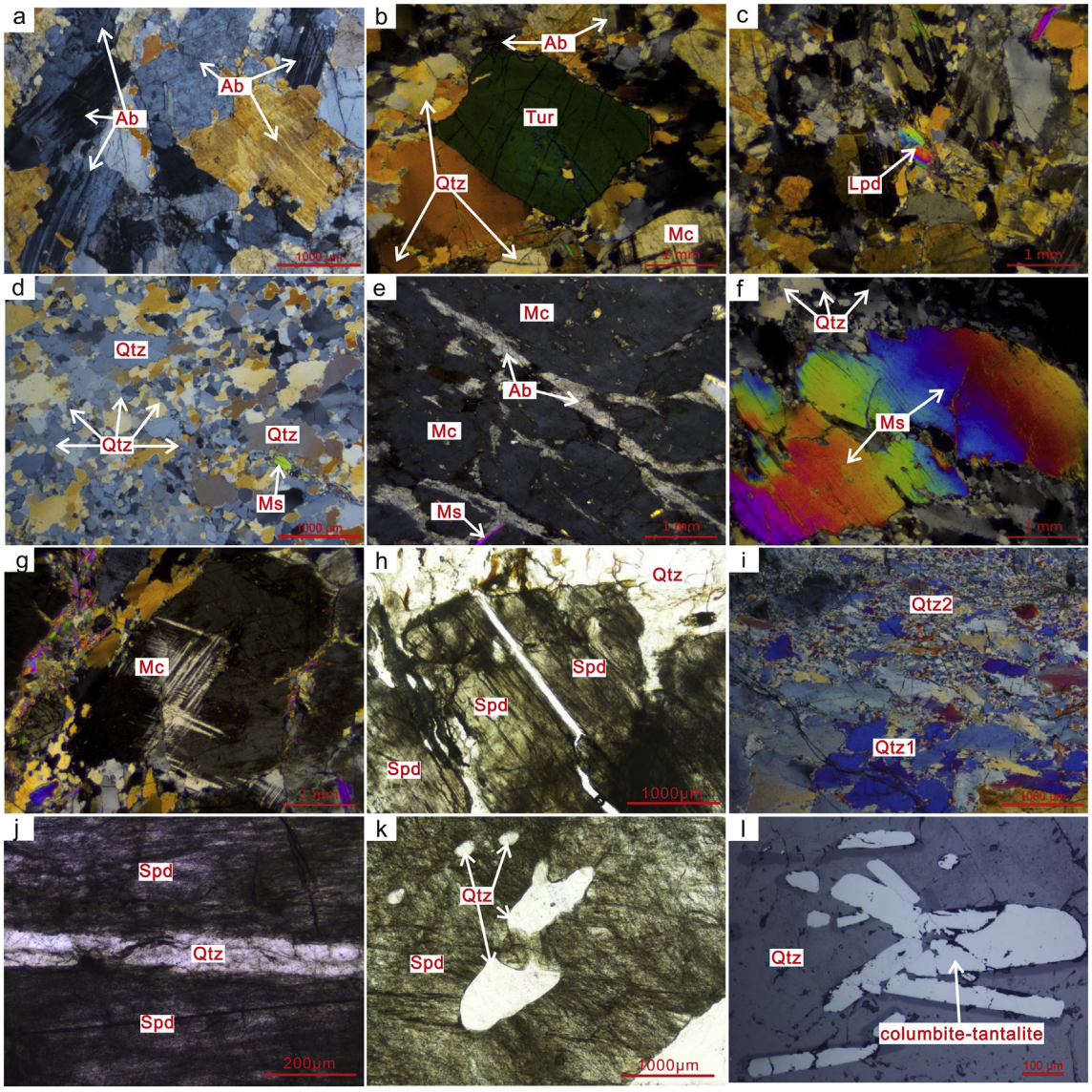

Fig. 3. Photomicrographs showing the characteristics and mineral assemblages of different zones in the Bailongshan pegmatite deposit. (a) Quartz with two different grain sizes in the quartz veins of the BFZ. (b) Coarse-grained muscovite in the QMZ. (c) Perthite in the BFZ consisting mainly of K-feldspar and minor albite. (d) Tourmaline in the FAZ. (e) Lepidolite in the FAZ. (f) Cross-hatched twinning in microcline. (g) Albite in the FAZ. (h) Columbite–tantalite in the SQZ (reflected light). (i) Two stages of quartz veins in the SQZ. (j) Tabular megacryst of spodumene surrounded by quartz and feldspar in the SQZ. (k) Late quartz veins cutting spodumene megacrysts in the SQZ. (l) Late quartz veins cutting spodumene megacrysts in the SQZ.

China. The thermocouples were calibrated over a temperature range of −196 to 600 °C using synthetic FIs. The precision of the temperature measurements is ±0.1 °C in the range from −100 to 25 °C, ±1 °C in the range from 25 to 400 °C, and ± 2 °C at >400 °C. The heating rate was generally 0.2–5 °C/min during the FI measurements, but was reduced to 0.1 °C/min near the freezing point and 0.2–0.5 °C/min near the homogenisation temperature, in order to accurately record the phase transformations.

3.3. Laser Raman microspectroscopy

Vapour and solid compositions of individual FIs were measured using a Horiba Xplora Laser Raman Microspectrometer at the Key Laboratory of Mineralogy and Metallogeny, Chinese Academy of Sciences, Guangzhou, China. An Ar^+ ion laser operated at 44 mW was used to produce a 532 nm excitation wavelength. The scanning range was 100–4000 cm^{-1}, with an accumulation time of 10 s for each scan. The spectral resolution was 0.65 cm^{-1}. The Raman shift of a monocrystalline piece of silicon was determined to be 520.7 cm^{-1} before the analyses.

3.4. Fluid inclusion data treatment

The salinities of aqueous FIs, expressed as wt% NaCl equivalent (equiv.), were estimated using the data of Bodnar (1994) for the NaCl–CO_2 system. We also estimated the salinities of halite daughter mineral-bearing FIs using the method of Lecumberri-Sanchez et al. (2012), based on the bubble dissolution and homogenisation temperatures. Salinities of the CO_2-bearing FIs were calculated using the equation given by Roedder (1984).

3.5. Hydrogen and oxygen isotopes

Hydrogen and oxygen isotope analyses were conducted at the Aoshi Analytical Testing Company Ltd., Guangzhou, China. Quartz samples from the four mineral zones were crushed to 40–60 mesh, then

handpicked under a binocular microscope. Quartz grains with mineral inclusions were discarded. Hydrogen isotope analysis was carried out after thermal decrepitation of the FIs, and reaction with zinc at 400 °C to produce H_2. The hydrogen was then analysed by mass spectrometry. The conventional BrF_5 method was used for the determination of oxygen isotopes. The accuracy of the hydrogen and oxygen isotope analyses was ±2‰ and ± 0.2‰, respectively. The conversion from $\delta^{18}O_{PDB}$ to $\delta^{18}O_{SMOW}$ is based on the formula: $\delta^{18}O_{SMOW} = 1.03086\times \delta^{18}O_{PDB} + 30.86$.

4. Fluid inclusion petrography

Recent efforts to model the cooling histories of some chemically evolved pegmatite dykes indicate they cooled quickly from the border to core zones (London, 2005). Quartz formed in two different stages (Q1 and Q2) in the SQZ, and Q1 formed at the same stage as spodumene, based on hand specimen and petrographic observations. Given the rapid crystallisation of the pegmatites, Q1 in the SQZ and spodumene may have crystallised at the same stage. The FIs in spodumene and Q1, which were both closely related to ore formation, were mainly analysed, but some inclusions from the other three zones were also analysed for comparison. In addition, some secondary inclusions representing post-mineralisation fluids were also analysed.

Quartz grains from the four mineral zones contain a wide variety of primary and secondary FIs. There are four types of primary FI: (1) two-phase liquid-rich L-type, (2) two-phase vapour-rich V-type, (3) three-phase daughter mineral-bearing S-type, and (4) three-phase (CO_2–H_2O–NaCl) or two-phase (CO_2-rich) C-type inclusions. Secondary FIs in quartz are also abundant and occur along healed fractures. The FIs in the spodumene are fairly abundant, but are only primary and C-type.

4.1. Fluid inclusions in quartz

4.1.1. L-type FIs

These are the most common FIs in all four mineral zones. Most of these FIs (size = 2–10 μm) are primary and distributed in clusters (Fig. 4b). They contain 10–20 vol% vapour, and are commonly ellipsoidal or negative crystal-shaped, and rarely irregular in shape. Secondary FIs occur only in the BFZ.

4.1.2. S-type FIs

These FIs are also widely distributed, but are less common than L-type FIs. They are primary, 8–12 μm in size, contain 5–10 vol% vapour phases, and are usually irregular in shape. All these FIs contain halite as a daughter mineral, which is cubic and 1–3 μm in size (Fig. 4a and e).

4.1.3. V-type FIs

These FIs are only found in the SQZ. The V-type FIs (size = 6–12 μm) are primary, ellipsoidal or negative crystal-shaped, distributed in clusters (Fig. 4f), and contain <30 vol% liquid.

4.1.4. C-type FIs

These FIs are only found in the QMZ and SQZ. The C-type FIs are two-phase at room temperature (20 °C), and CO_2 bubbles appear at >10 °C. They are primary FIs (size = 5–10 μm), ellipsoidal or negative crystal-shaped, distributed in clusters (Fig. 4d), and contain <30 vol% liquid.

4.2. Fluid inclusions in spodumene

Numerous FIs occur along the cleavages of spodumene (Fig. 4c). All these FIs are negative crystal-shaped and the long axis is much larger than the short axis. At room temperature, these FIs are two-phase and similar to C-type FIs in quartz (Fig. 4g–h). The CO_2 phase ranges widely from 20 to 80 vol% (Fig. 4i).

5. Results

5.1. Fluid inclusion microthermometry

In the FAZ and BFZ, ice melting temperatures of the L-type FIs are −20.5 to −11.4 and − 6.9 to −2.9 °C, with corresponding salinities of 15.4–22.7 and 4.8–10.4 wt% NaCl equiv., and homogenisation temperatures of 283–338 and 156–224 °C, respectively. The halite melting temperatures of S-type FIs in the FAZ are 96–230 °C, and these FIs homogenised at 183–285 °C (Table 1, Fig. 5).

In the SQZ (Fig. 6), melting of solid CO_2 occurred at −57.2 to −56.8 °C. The melting temperatures of CO_2 clathrate varied from 2.4–7.7 °C, corresponding to salinities of 4.4–12.6 wt% NaCl equiv. These FIs homogenised at 234–286 °C. The salinities of the L-type FIs in quartz vary from 10.5–22.1 wt% NaCl equiv., and the homogenisation temperatures ranged from 223 to 421 °C. Salinities of S-type FIs in quartz are 26.6–30.6 wt% NaCl equiv., and these FIs homogenised at 214–298 °C. For the 25 primary C-type FIs in spodumene that were analysed, melting of solid CO_2 occurred at −58.6 to −57.9 °C. The melting temperatures of CO_2 clathrate varied from −2.8 to 5.3 °C, corresponding to FI salinities of 8.5–18.1 wt% NaCl equiv. These FIs homogenised at 256–321 °C. Notably, critical homogeneity was observed in C-type FIs in spodumene (i.e., the volume of gas and liquid phases only slightly changed or was unchanged during heating). When the temperature reached the homogenisation temperature, the gas–liquid interface became unclear and disappeared, resulting in formation of a homogeneous fluid phase (Shi, 1987).

5.2. Laser Raman spectroscopy

Representative FIs in all four zones were systematically measured using laser Raman spectroscopy. The vapour phase consists primarily of water in the FAZ and BFZ. Water is also the main component in the vapour phase of L-type FIs in the QMZ, and V-type FIs show the characteristic peak of CO_2 (1384 cm^{-1}; Fig. 7c). In the analysed quartz, spectral peaks of CO_2, N_2, and CH_4 were found in C-type FIs (Fig. 7a); however, the vapour phase in the other types of FIs comprise mainly water (Fig. 7b). In the analysed spodumene, the C-type FIs have the same spectral peaks as the C-type FIs in quartz (Fig. 7d).

5.3. Hydrogen and oxygen isotopes

Hydrogen and oxygen isotope data were obtained for quartz from the four zones (Fig. 8). Quartz grains from the FAZ (border zone) have $\delta^{18}O_{V\text{-}SMOW}$ = 9.6‰–10.2‰, while those from the BFZ and QMZ (wall zone) have $\delta^{18}O_{V\text{-}SMOW}$ = 8.6‰–8.9‰. Mineralised quartz grains in the SQZ have $\delta^{18}O_{V\text{-}SMOW}$ = 9.0‰–9.2‰. The δD values vary widely, and the FAZ has δD = −38‰ to 107‰, while the BFZ and QMZ has δD = −56‰ to −107‰. Mineralised quartz grains in the SQZ have δD = −77‰ to −81‰.

6. Discussion

6.1. Compositions and characteristics of the ore-forming fluids

London et al. (1989) suggested that crystallisation of a pegmatite is a rapid, disequilibrium, and stepwise process. Fuertes-Fuente et al. (2000b) showed that the trapping conditions of FIs did not vary from the wall to core zone of a pegmatite in the Black Hills, USA. Ackerman et al. (2007) found that the formation pressure of Li-bearing pegmatites is lower than that of associated barren pegmatites.

6.1.1. Salinity, temperature, and pressure

FIs with halite crystals are common in the four mineral zones. The fluid salinities are 26.6–33.5 wt% NaCl equiv. (S-type FIs), 15.4–22.7 wt% NaCl equiv. (L-type FIs), 4.4–18.1 wt% NaCl equiv.

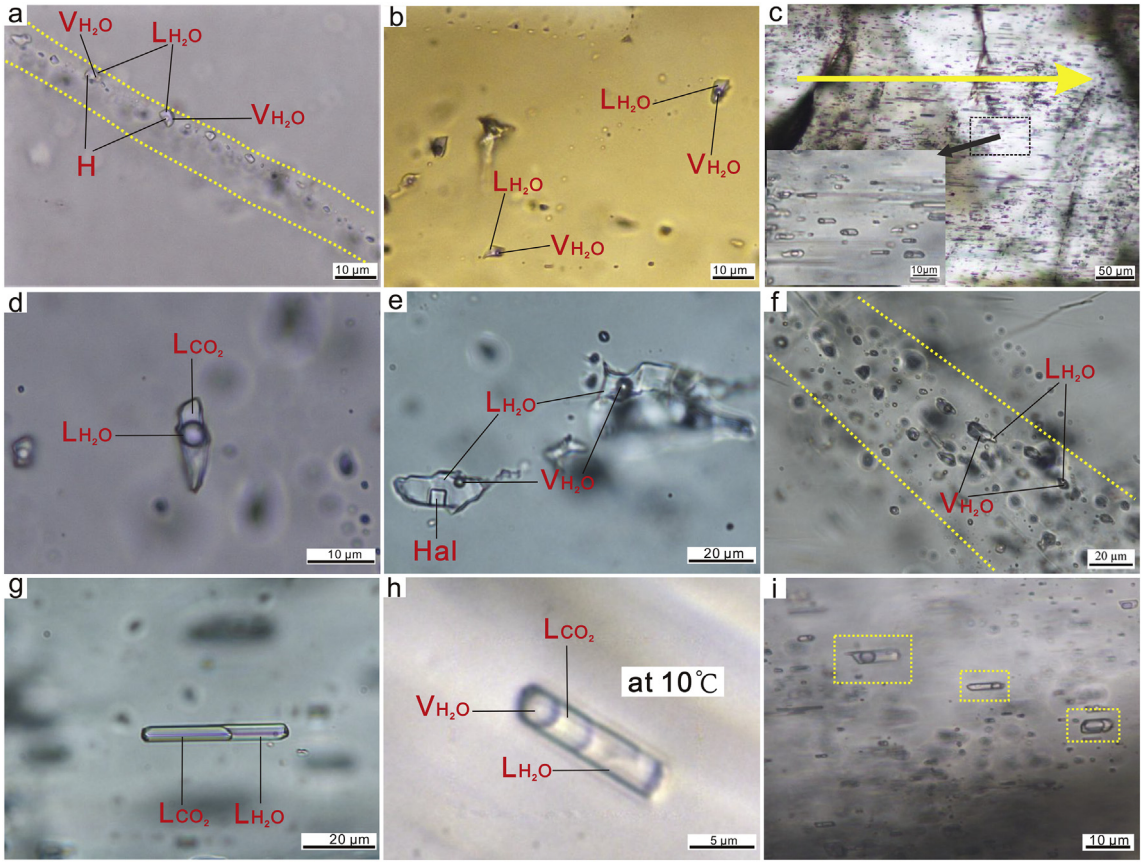

Fig. 4. Photomicrographs of FIs in the Bailongshan pegmatite deposit. (a) Primary FIs growing along the cleavage in spodumene. (b) Multiphase secondary FIs in the BMZ. (c) V-type FIs with V_{H2O} and L_{H2O} in the SQZ. (d) C-type FIs with L_{H2O} and L_{CO2} in quartz from the SQZ. (e) C-type FIs with L_{H2O} and L_{CO2} in quartz from the QMZ. (f) S-type FIs with V_{H2O}, L_{H2O}, and halite daughter minerals, with the FIs exhibiting obvious deformation and necking. (g) C-type negative-crystal FIs with L_{H2O} and L_{CO2} in spodumene from the SQZ. (h) S-type FIs with halite daughter minerals in the FAZ. (i) The volume of C-type FIs in spodumene. Abbreviations: V_{H2O} = H_2O vapour; L_{H2O} = H_2O liquid; L_{CO2} = CO_2 liquid; Hal = halite.

(C-type FIs), and 4.8–10.4 wt% NaCl equiv. (secondary FIs in the BFZ). The FI homogenisation temperatures are clearly different in each zone and in different FI types in a particular zone. The homogenisation temperatures of L-, S-, and C-type FIs in quartz (mainly 230–320 °C) are considerably lower than those of the FIs in spodumene, but higher than those of secondary FIs in the BFZ (180–210 °C). Given these FI data, the ore-forming fluids were likely of medium–low-salinity and medium–low-temperature. We found no discernible variations in fluid salinity and temperature in each of these four zones. We suggest that the FIs were trapped from discrete batches of fluids (with different salinities and homogenisation temperatures) during fractional crystallisation of the pegmatite.

According to the mineral assemblage phase diagram of Burnham and Nekvasil (1986), Li-bearing pegmatite forms a K-feldspar–albite–quartz–spodumene–dolomite mineral assemblage (without petalite) between 2 and 5 kbar. Based on petrography, the Bailongshan pegmatite belongs to the spodumene-subtype of the rare-element–Li type, which typically forms at 3–4 kbar (Černý and Ercit, 2005; Landsman, 1984). Using the homogenisation temperatures of CO_2 in C-type FIs, the CO_2 density in the spodumene was calculated as 0.68–0.91 using the T–W–ρ phase diagram (Bodnar, 1983). Based on the homogenisation temperatures (256–321 °C) and CO_2 densities, the pressure was estimated to be 1.90–3.75 kbar (Fig. 9; Brown and Lamb, 1989; Cheng et al., 2020). As such, we speculate that the ore-forming pressure of the Bailongshan pegmatite deposit was 3.00–3.75 kbar, corresponding to a mineralisation depth of 9–11 km (i.e., assuming 30 MPa/km).

Table 1
Microthermometric results of fluid inclusions from the Bailongshan deposit.

Zone	Host mineral	FI type/shape	Size (μm)	Tm, CO_2/°C	Th, CO_2/°C	Tm, ice/°C	Tm, halite/°C	Th, total/°C	Salinity (wt% NaCl eqv.)
FAZ	Quartz	L-type; ellipse or negative crystal	2–4			−11.4 to −20.5		283–338 (9)	15.4–22.7
	Quartz	S-type; Polygonal or irregular	3–8				96–230	183–285 (8)	27.7–33.5
BFZ	Early-stage quartz	L-type; irregular or negative crystal	5–8			−2.9 to −6.9		156–224 (12)	4.8–10.4
SQZ	Early-stage quartz	L-type; irregular	3–10			−7.0 to −19.6		223–421 (15)	10.5–22.1
	Early-stage quartz	S-type; irregular	4–8				35.2–175	214–298 (6)	26.7–30.6
	Early-stage quartz	C-type, polygonal or rhombic	5–8	−57.2 to −56.8	+2.4 to +7.7			234–286 (9)	4.4–12.6
	Spodumene	C-type; negative crystalline,	5–20	−57.9 to −58.6	+7.5 to +27.5			256–321 (25)	8.5–18.1

Note: 1) numbers in brackets are fluid inclusions measured. 2) Tm, CO_2: melting temperature of solid CO_2; Th, CO_2: CO_2 partial homogenisation temperature; Tm, ice: melting temperature of ice; Tm, halite: melting temperature of halite; Th: homogenisation temperature.

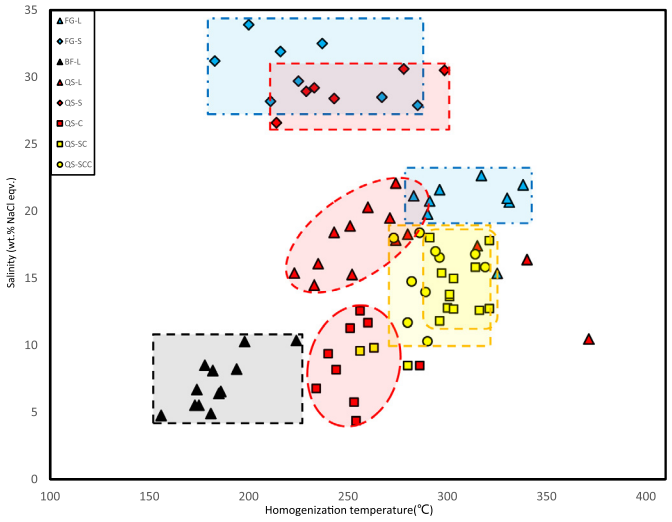

Fig. 5. Plot of homogenisation temperatures vs. salinities for FIs in the Bailongshan pegmatite deposit. Abbreviations: FG-L = L-type FIs in the FAZ; FG-S = S-type FIs in the FAZ; BF-L = L-type FIs in the BFZ; QS-L = L-type FIs in quartz from the SQZ; QS-S = S-type FIs in quartz from the SQZ; QS-C = C-type FIs in quartz from the SQZ; QS-SC = C-type FIs in spodumene from the SQZ; QS-SCC = C-type critical FIs in spodumene from the SQZ.

6.1.2. CO_2 and carbonic inclusions

Most rare-metal pegmatites worldwide contain abundant CO_2-bearing FIs (Fuertes-Fuente et al., 2000a; London, 1985; Lowenstern, 2001; Thomas et al., 2009). CO_2 can enhance immiscibility and independent gas phase separation, and has a key role in the formation and evolution of metal-bearing complexes (Lowenstern, 2001). Spycher and Reed (1989) calculated and simulated the boiling process of epithermal ore-forming fluids, which showed that CO_2 degassing leads to a fluid pH increase and base metal precipitation (Ertan and Leeman, 1999; Lowenstern, 2001; Scambelluri and Philippot, 2001). The abundant C-type inclusions in spodumene and quartz in the SQZ indicate that CO_2 was closely related to the ore-forming fluids.

The trapping pressure of C-type FIs in the SQZ quartz (2.1–3.1 kbar) is lower than that of the FIs in spodumene (1.90–3.75 kbar; Fig. 9). Homogenisation temperatures of C-type FIs in quartz (234–286 °C) are generally lower than those of C-type FIs in spodumene (256–321 °C). It is clear that the average homogenisation temperatures of aqueous FIs with high salinity and primary C-type FIs in quartz are lower than those of primary C-type FIs in spodumene. We speculate that, during spodumene crystallisation, as the temperature–pressure and solubility of CO_2 and H_2O–NaCl decreased, gradual CO_2 saturation and separation from the ore-forming fluids occurred. This might have resulted in the FIs evolving from a medium–low-salinity H_2O–CO_2–NaCl system to a medium–high-salinity H_2O–NaCl system and to a low-salinity H_2O–CO_2–NaCl system. This process is typical for Li-bearing pegmatite deposits worldwide, such as the Ketohai (China; Lu et al., 1996) and Tanco (Canada) deposits (London, 1986).

6.2. Ore formation mechanisms

6.2.1. Supercritical fluid

Of the 25 primary FIs in spodumene, 10 are critical (Fig. 10; Shi, 1987), and are all primary FIs of medium–low-salinity. The homogenisation temperatures and trapping pressures of the other types of FIs in spodumene are not significantly different from those of the critical FIs, indicating that the timing of fluid trapping was similar. This indicates that the Bailongshan ore-forming fluids were low-salinity critical and supercritical CO_2-rich fluids.

Given their high solubility and diffusivity, supercritical fluids are considered to be important in the formation of (super) large ore deposits. These fluids can effectively leach ore-forming materials from source rocks and transport these materials in the form of organic complexes (Ajzenberg et al., 2000; Giordano, 1994; Xiao and Fan, 2001). Where the mineralisation is related to granite, the addition of supercritical fluids favours the formation of complex anion groups associated with highly coordinated cations, such as ore-forming elements (Qiu

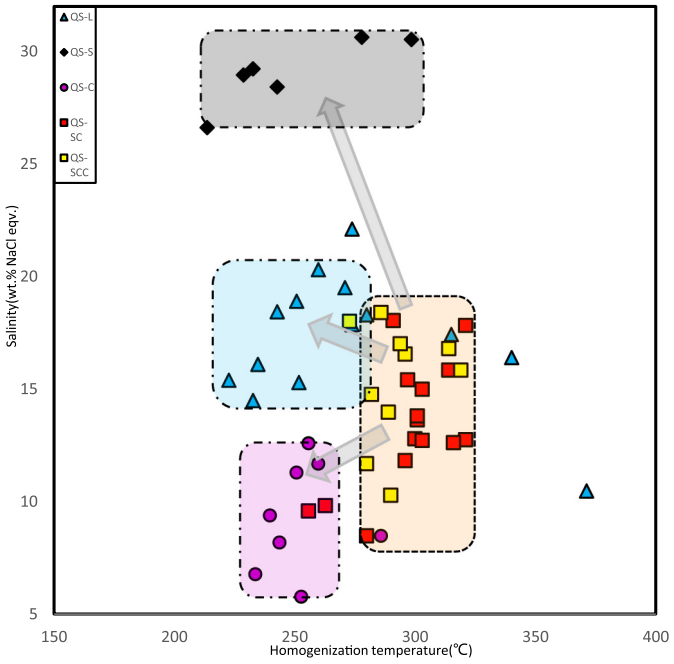

Fig. 6. Plot of homogenisation temperatures vs. salinities for FIs in the SQZ. CO_2–H_2O–NaCl FIs gradually transition to H_2O–NaCl FIs. Abbreviations: QSL = L-type FIs in quartz; QSS = S-type FIs in quartz; QSSC = C-type FIs in spodumene; QSSCC = C-type critical FIs in spodumene.

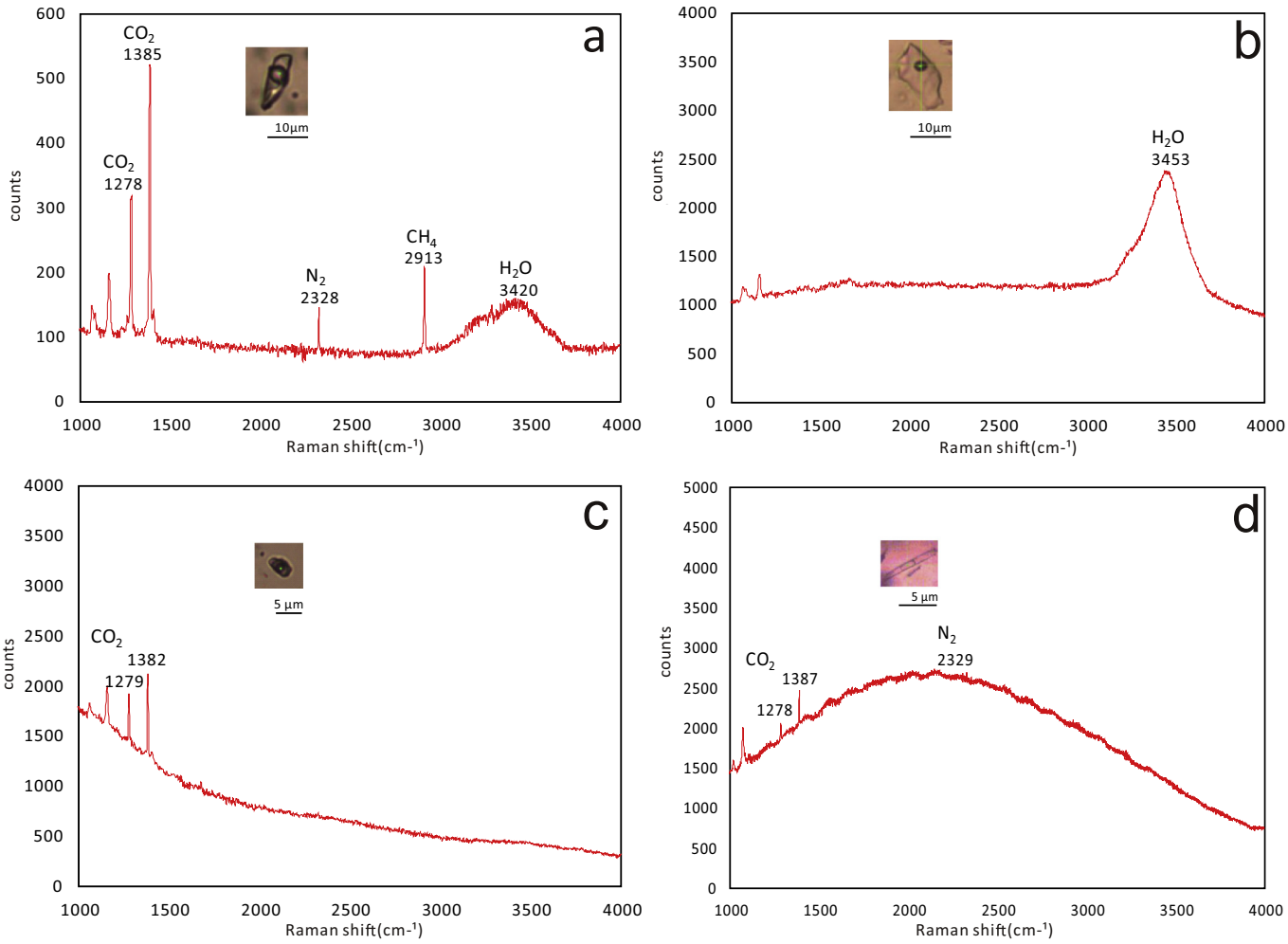

Fig. 7. Laser Raman spectra of the FIs. (a) CO_2 and H_2O peaks in fluid in a C-type FI in spodumene from the SQZ. N_2 and CH_4 peaks are also present. (b) H_2O peaks in vapour in a L-type FI in quartz from the SQZ. (c) CO_2 peaks in fluid in a C-type FI in quartz from the SQZ. (d). CO_2 and N_2 peaks in fluid in a C-type FI in spodumene from the SQZ.

et al., 1998; Qiu and Peng, 1997). Changes in the fluid chemistry caused by temperature and pressure variations near the critical point of water is important in the formation of superlarge polymetallic ore deposits (Shi, 1987; Wen and Mao, 2002), which likely occurred in the case of the Bailongshan superlarge pegmatite deposit.

6.2.2. Fluid boiling

Trapping pressures of the SQZ C-type FIs varied widely (i.e., distinct pressure changes in the system occurred during spodumene crystallisation). The volume of CO_2 in the C-type FIs has a wide range of 10–80 vol%, which is evidence of fluid boiling (Fig. 4i). However, these characteristics cannot definitively verify whether this is a boiling FI group, and this must be further assessed using homogenisation temperature data (Lu et al., 1996). We selected FIs with different CO_2 volumes in the same crystal for measurement of the homogenisation temperatures. Most of the FIs with smaller volumes of CO_2 were homogenised to the liquid phase, and all the FIs with larger volumes of CO_2 were homogenised to the gas phase. In Q1, most of the original primary FIs are irregular in shape, with obvious necking or deformation (Fig. 4e), which further indicates abrupt pressure changes and boiling.

Fluid boiling is one of the most important mechanisms for ore formation in magmatic–hydrothermal deposits (including pegmatite deposits; Roedder, 1984). Fluid boiling is mainly caused by: (1) contact with meteoric water that causes a temperature drop, or (2) a pressure drop when fluids enter open structures (Zhang, 1997). Our oxygen isotope data show that there was no mixing with meteoric water or other external fluids (see below), which excludes the first possibility. The second possibility appears more plausible due to the presence of five large faults in the Bailongshan deposit, along with well-developed fractures

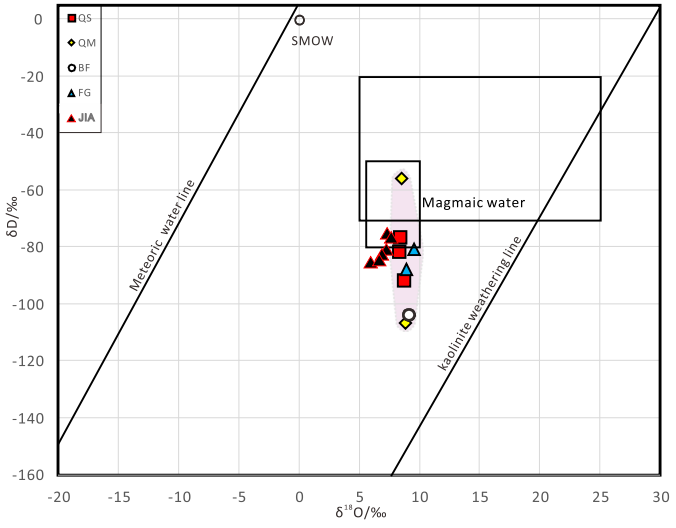

Fig. 8. H–O isotopic compositions of the Bailongshan and Jiajika pegmatite deposits (Li et al., 2006). Fields for primary magmatic and metamorphic waters are from Taylor (1974). Abbreviations: JIA = Jiajika pegmatite deposit.

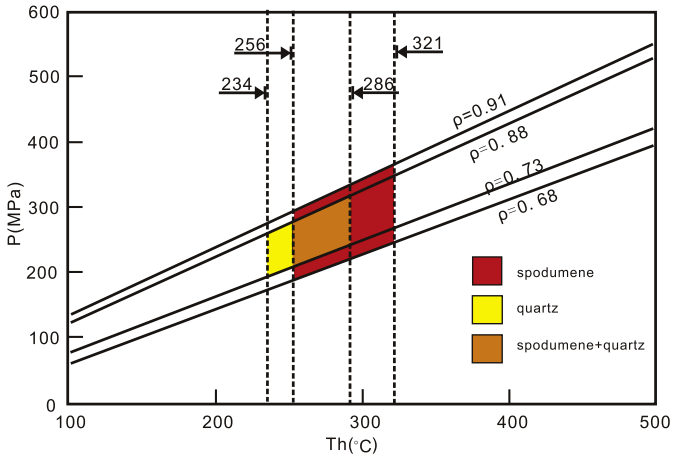

Fig. 9. Estimated trapping pressures and temperatures for the Bailongshan pegmatite deposit. Isochores for the C-type FIs were calculated using the Flincor software.

and joints (Wang et al., 2017). Therefore, we speculate that the fluid pressure drop was structurally controlled, and resulted in CO_2 exsolution.

6.2.3. Metallogenic mechanism

Li and Chou (2017) experimentally showed that a carbonic aqueous fluid can transport ore-forming elements rich in silica and alkali metals to the crystallisation front of a pegmatite. Its composition appears to be similar to that of hydrosilicate liquids, with a low viscosity and high element diffusion and mass transport capacity, which enables extreme enrichments of lithophile metals like lithium. This provides useful insights into formation models of rare-metal pegmatites. In a high-temperature and CO_2-rich fluid system, SiO_2 can be dissolved in aqueous solutions that are alkali- and carbonate-rich as alkaline bisilicate. In this carbonic aqueous fluid, Li^+ is mainly transported as $LiHCO_3$ or Li_2CO_3.

The abundant C-type FIs in spodumene indicate that CO_2 was supersaturated during ore precipitation, which supports our suggestion that spodumene crystallised from a Li- and carbonate-rich fluid (Thomas et al., 2011a). In such a fluid system, zabuyelite (Li_2CO_3) is often preserved as a daughter mineral in FIs, but is actually rare (Thomas et al., 2011a). We did not identify zabuyelite in FIs in our samples. However, at high temperatures, zabuyelite will dissolve in aqueous solutions that are alkali- and carbonate-rich (Thomas et al., 2011b) via the following reaction (Li and Chou, 2017):

$$2LiHCO_3 + 2SiO_2 \rightarrow Li_2Si_2O_5 + 2CO_2 + H_2O$$

Ore formation may be caused by a sudden drop in pressure, which affects the solubility and diffusivity of elements in supercritical fluids. In the $LiAlSiO_4$–SiO_2–H_2O system considered by London (2008), the quartz-saturated stability relationships among the Li-bearing minerals are only a function of temperature and pressure. We have shown that the ore-forming pressure of the Bailongshan pegmatite deposit was 3.00–3.75 kbar, thus the ore-forming fluid temperature was <600 °C. The decrease in pressure would have inevitably led to the loss of CO_2, rapid decrease in temperature, and reduced solubility of Li^+. Extensive ore precipitation would then have formed most of the spodumene ores and primary FIs.

6.3. Fluid source and evolution

The $\delta^{18}O$ values of S- and I-type granites are generally >10‰ and < 10‰ (mostly 8‰–9‰), respectively (Černý and Ercit, 2005). The $\delta^{18}O$ values of quartz in each zone cluster at 8.9‰ ± 0.8‰, indicating there were no isotopic changes during fluid evolution. The fluids may have been derived mainly from the differentiation and evolution of the pegmatitic magma with no external input, at least in the early and main mineralisation stages.

The δD values vary widely in the Bailongshan pegmatite deposit, but show no systematic trends. Later-formed hydroxyl-bearing igneous minerals record the isotopic composition of the degassed melt, rather than the melt prior to degassing, which may be responsible for the observed δD variations (Hoefs, 1997).

Xu et al. (2018) suggested that the Dahongliutan area underwent post-orogenic extension, which resulted in partial melting of the crust and formation of granites in this area. During the late stages of evolution of a granite magma chamber, the residual hydrothermal fluid may become enriched in ore elements and form pegmatites. The Tianshuihai and Songpan–Ganzi blocks might have been connected (Wang et al., 2004), and the Bailongshan and Jiajika pegmatite deposits were likely formed in the same tectonic setting. The FIs in spodumene in the Jiajika and Bailongshan pegmatites are quite different, but the oxygen isotopic characteristics of the two deposits are similar (Fig. 8). The fluids of the Jiajika pegmatite may have been post-magmatic hydrothermal fluids from the granite (Li et al., 2006a, 2006b).

We suggest that the Bailongshan ore-forming fluids might have been sourced from residual granitic melts, which were originally formed by partial melting of the continental crust. No discernible external fluid input is evident in the early and main stages of mineralisation at Bailongshan.

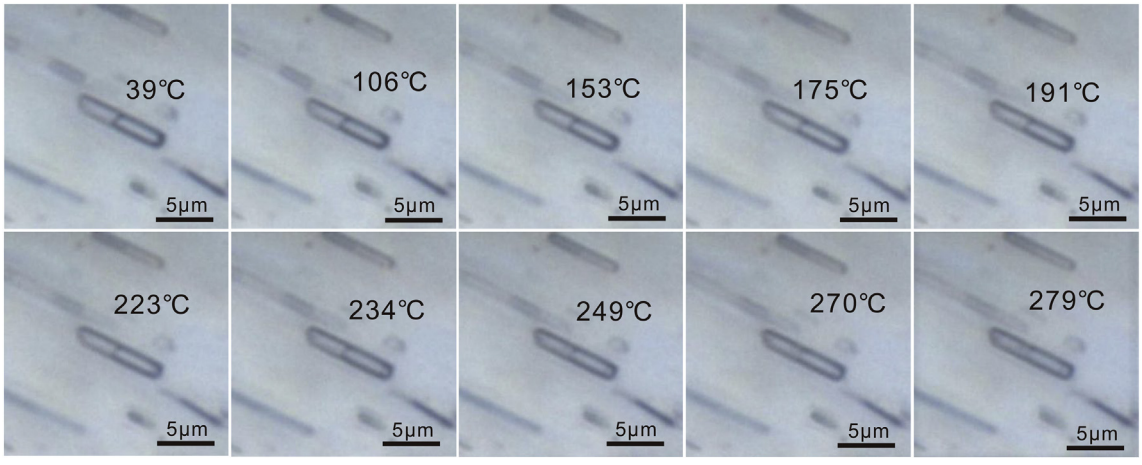

Fig. 10. Critical homogenisation of a C-type inclusion in spodumene during heating. Homogeneity of the CO_2 phase was reached by 39 °C, and critical homogeneity was reached at 279 °C.

The Bailongshan ore-forming fluids were low-temperature, low–medium-salinity, and rich in volatiles such as CO_2 (along with minor CH_4 and N_2). Our FI study identified no obvious trends in the fluid temperature and salinity in each mineral zone, which is consistent with rapid and continuous crystallisation of the pegmatites. Fluid boiling and degassing might have occurred when the fluids entered open structures, such as the many faults and fractures in the mining area. This likely led to an abrupt decrease in Li^+ solubility in the fluids, and thus ore precipitation. The pressure drop also likely led to the separation of CO_2 from the fluids and formed the H_2O–NaCl FIs (with higher salinity) and CO_2-rich FIs (with lower salinity).

7. Conclusions

1. The ore-forming fluids of the Bailongshan Li–Rb deposit were low–medium-temperature (183–421 °C), low–medium-salinity (4.4–30.6 wt% NaCl equiv.), contained abundant CO_2, and were supercritical.
2. The ore-forming fluids were derived by the fractionation of pegmatitic magma and did not contain meteoric water input. The fluid trapping pressure was 3.00–3.75 kbar, which is equivalent to mineralisation depths of 9–11 km.
3. Supercritical fluids might have contributed to the enrichment of ore-forming elements in the fluids, and fluid boiling might have led to CO_2 degassing and Li ore formation.

Declaration of Competing Interest

We declare that we have no financial and personal relationships with other people or organizations that can inappropriately influence our work, there is no professional or other personal interest of any nature or kind in any product, service and/or company that could be construed as influencing the position presented in, or the review of, the manuscript entitled.

Acknowledgements

This research was supported by the National Science Foundation for Young Scientists of China (Grant 41702085) and the National Key R&D Program of China (Grant 2016YFC0600403). We sincerely thank He Wang from the Guangzhou Institute of Geochemistry, Chinese Academy of Sciences, for constructive suggestions on our research. This is contribution No.IS-2916 from GIGCAS.

References

Abella, P.A., Draper, J.C.M.I., Cordomi, M.C.I., 1995. Nb–Ta-minerals from the Cap de Creus pegmatite field, eastern Pyrenees: distribution and geochemical trends. Mineral. Petrol. 55 (1), 53–69.

Ackerman, L., Zachariáš, J., Pudilová, M., 2007. P–T and fluid evolution of barren and lithium pegmatites from Vlastějovice, Bohemian Massif, Czech Republic. Int. J. Earth Sci. 96 (4), 623–638.

Ajzenberg, N., Trabelsi, F., Recasens, F., 2000. What's new in industrial polymerization with supercritical solvents? A short review. Chem. Eng. Technol. 23 (10), 829–839.

Anderson, A.J., Gray, S., Clark, A.H., 2001. The occurrence and origin of zabuyelite (Li_2CO_3) in spodumene-hosted fluid inclusions: Implications for the internal evolution of rare-element granitic pegmatites. Can. Mineral. 39 (3), 1513–1527.

Bartels, A., Behrens, H., Holtz, F., Schmidt, B., Fechtelkord, M., Knipping, J., Crede, L., Baasner, A., Pukallus, N., 2013. The effect of fluorine, boron and phosphorus on the viscosity of pegmatite forming melts. Chem. Geol. 346, 184–198.

Bartels, A., Behrens, H., Holtz, F., Schmidt, B.C., 2015. The effect of lithium on the viscosity of pegmatite forming liquids. Chem. Geol. 410, 1–11.

Bodnar, R.J., 1983. A method of calculating fluid inclusion volumes based on vapor bubble diameters and P–V–T–X properties of inclusion fluids. Econ. Geol. 78 (3), 535–542.

Bodnar, R.J., 1994. Synthetic fluid inclusions: XII. The system H_2O–NaCl. Experimental determination of the halite liquidus and isochores for a 40 wt.% NaCl solution. Geochim. Cosmochim. Acta 58 (3), 1053–1063.

Brown, P., Lamb, W., 1989. P–V–T properties of fluids in the system $H_2O \pm CO_2 \pm$ NaCl: New graphical presentations and implications for fluid inclusion studies. Geochim. Cosmochim. Acta 53 (6), 1209–1221.

Burnham, C.W., Nekvasil, H., 1986. Equilibrium properties of granite pegmatite magmas. Am. Mineral. 71 (3–4), 239–263.

Černý, P., 1991. Fertile granites of Precambrian rare-element pegmatite fields: is geochemistry controlled by tectonic setting or source lithologies? Precambrian Res. 51 (1–4), 429–468.

Černý, P., Ercit, T., 2005. The classification of granitic pegmatites revisited. Can. Mineral. 43 (6), 2005–2026.

Cheng, X., Xu, J., Yang, F., Zhang, G., Zhang, H., Bian, C., Xue, Q., 2020. New constraints on the genesis and geodynamic setting of the Wulong gold deposit, Liaodong Peninsula, NE China: evidence from geology, geochemistry, fluid inclusions and C–H–O–S–Pb isotopes. Can. J. Earth Sci. 57 (3), 307–330.

Ertan, I., Leeman, W., 1999. Fluid inclusions in mantle and lower crustal xenoliths from the Simcoe volcanic field, Washington. Chem. Geol. 154 (1–4), 83–95.

Frezzotti, M., Di Vincenzo, G., Ghezzo, C., 1994. Evidence of magmatic CO_2-rich fluids in peraluminous graphite-bearing leucogranites from Deep Freeze Range (northern Victoria Land, Antarctica). Petrology 117 (2), 111–123.

Fuertes-Fuente, M., Martin-Izard, A., Boiron, M., Mangas, J., 2000a. Fluid evolution of rare-element and muscovite granitic pegmatites from central Galicia, NW Spain. Mineral. Deposita 35 (4), 332–345.

Fuertes-Fuente, M., Martin-Izard, A., Boiron, M.C., Vinuela, J.M., 2000b. P–T path and fluid evolution in the Franqueira granitic pegmatite, central Galicia, northwestern Spain. Can. Mineral. 38 (5), 1163–1175.

Ghavidel-syooki, M., Mohammad, G., Leonid, P., Mansoureh, G., José-Javier, A., 2015. Late Ordovician and early Silurian brachiopods from the Zagros Ranges, Iran. Earth Environ. Sci. Trans. R. Soc. Edinburgh 105, 1–29.

Giordano, T., 1994. Metal transport in ore fluids by organic ligand complexation. In: Pittman, E.D., Lewan, M.D. (Eds.), Organic Acids in Geological Processes. Springer, Berlin Heidelberg, Berlin, Heidelberg, pp. 319–354.

Hoefs, J., 1997. Variations of Stable Isotope Ratios in Nature. Springer, Berlin, Heidelberg, p. 106.

Kesler, S., Gruber, P.W., Medina, P., Keoleian, G., Everson, M., Wallington, T., 2012. Global lithium resources: relative importance of pegmatite, brine and other deposits. Ore Geol. Rev. 48, 55–69.

Landsman, D., 1984. Experimental phase equilibria in the system $LiAlSiO_4$–SiO_2–H_2O: a petrogenetic grid for lithium-rich pegmatites. Am. Mineral. 69 (11−12), 995–1004.

Lecumberri-Sanchez, P., Steele-MacInnis, M., Bodnar, R.J., 2012. A numerical model to estimate trapping conditions of fluid inclusions that homogenize by halite disappearance. Geochim. Cosmochim. Acta 92, 14–22.

Li, J., Chou, I., 2017. Homogenization experiments of crystal-rich inclusions in spodumene from Jiajika lithium deposit, China, under elevated external pressures in a hydrothermal diamond-anvil cell. Geofluids 2017, 1–12.

Li, J., Wang, H., Zhang, D., Fu, X., 2006a. The discovery of silicate daughter mineral-bearing inclusions in the Jiajika pegmatite deposit, western Sichuan, and its significance. Mineral Deposits 25, 131–134.

Li, J., Wang, H., Zhang, D., Fu, X., 2006b. The source of ore-forming fluid in Jiajika pegmatite type lithium polymetallic deposit, Sichuan Province. Acta Petrol. Mineral. 25 (1), 45–52.

Liu, L., Wang, D., Liu, X., Li, J., Dai, H., Yan, W., 2017. The main types, distribution features and present situation of exploration and development for domestic and foreign lithium mine. Geol. China 44, 263–278.

London, D., 1985. Origin and significance of inclusions in quartz; a cautionary example from the Tanco Pegmatite, Manitoba. Econ. Geol. 80 (7), 1988–1995.

London, D., 1986. Magmatic–hydrothermal transition in the Tanco rare-element pegmatite: evidence from fluid inclusions and phase-equilibrium experiments. Am. Mineral. 71 (3–4), 376–395.

London, D., 1987. Internal differentiation of rare-element pegmatites: Effects of boron, phosphorus, and fluorine. Geochim. Cosmochim. Acta 51 (3), 403–420.

London, D., 1990. Internal differentiation of rare-element pegmatites; a synthesis of recent research. Geol. Soc. Am. Spec. Pap. 246, 35–50.

London, D., 2005. Granitic pegmatites: an assessment of current concepts and directions for the future. Lithos 80 (1–4), 281–303.

London, D., 2008. Pegmatites. 10. The Canadian Mineralogist, Ottawa Special Publication.

London, D., 2018. Ore-forming processes within granitic pegmatites. Ore Geol. Rev. 101, 349–383.

London, D., Morgan, G.B., Hervig, R.L., 1989. Vapor-undersaturated experiments with Macusani glass+H_2O at 200 MPa, and the internal differentiation of granitic pegmatites. Contrib. Mineral. Petrol. 102 (1), 1–17.

Lowenstern, J.B., 2001. Carbon dioxide in magmas and implications for hydrothermal systems. Mineral. Deposita 36 (6), 490–502.

Lu, H., Wang, Z., Li, Y., 1996. Magma/fluid transition and genesis of pegmatite dike No. 3 at Altay, Xinjiang. Acta Mineral. Sin. 16, 1–7.

Mattern, F., Schneider, W., Li, Y., Li, X., 1996. A traverse through the western Kunlun (Xinjiang, China): tentative geodynamic implications for the Paleozoic and Mesozoic. Geol. Rundsch. 85 (4), 705–722.

Nabelek, P., Gammel, E., 2016. Fluid inclusion examination of the transition from magmatic to hydrothermal conditions in pegmatites from San Diego County, California. Am. Mineral. 101, 1906–1915.

Nabelek, P.I., Whittington, A.G., Sirbescu, M.L.C., 2010. The role of H_2O in rapid emplacement and crystallization of granite pegmatites: resolving the paradox of large crystals in highly undercooled melts. Contrib. Mineral. Petrol. 160 (3), 313–325.

Qiu, R., Peng, S., 1997. Genesis of granitic Nb–Ta deposit in Xianghualing area and the role of the supercritical fluid in the process of rock-forming and mineralization. Hunan Geol. 16, 92–97.

Qiu, R., Zhou, X., Chang, H., Du, S., 1998. Role of the supercritical fluid in the process of granitic rock-forming and mineralization: taking the granitic Nb–Ta deposit in Xianghualing area as an example. Geol. Sci. Technol. Inf. 17, 41–45.

Redden, J., Norton, J., 1990. Relations of zoned pegmatites to other pegmatites, granite, and metamorphic rocks in the southern Black Hills, South Dakota. Am. Mineral. 75 (5), 631–655.
Roedder, E., 1984. Fluid Inclusions. Reviews in Mineralogy. 12. Mineralogical Society of America (644 pp.).
Scambelluri, M., Philippot, P., 2001. Deep fluids in subduction zones. Lithos 55 (1–4), 213–227.
Shi, L., 1987. Critical inclusions and supercritical fluid in minerals and their metallogenesis. Geol. Prospect. 23, 36–40.
Smerekanicz, J.R., Francis, Ö.D., 1999. Reconnaissance fluid inclusion study of the Morefield pegmatite, Amelia County, Virginia. Am. Mineral. 84 (5–6), 746–753.
Smirnov, S.Z., 2015. The fluid regime of crystallization of water-saturated granitic and pegmatitic magmas: a physicochemical analysis. Russ. Geol. Geophys. 56, 1292–1307.
Spycher, N.F., Reed, M.H., 1989. Evolution of a Broadlands-type epithermal ore fluid along alternative P–T paths; implications for the transport and deposition of base, precious, and volatile metals. Econ. Geol. 84 (2), 328–359.
Stewart, D.B., 1978. Petrogenesis of lithium-rich pegmatites. Am. Mineral. 63, 970–980.
Thomas, M., Williams, J., 2018. The physical and chemical evolution of fluids in rare-element granitic pegmatites associated with the Lacorne pluton, Québec, Canada. Chem. Geol. 493, 281–297.
Thomas, R., Davidson, P., Badanina, E.J.M., 2009. A melt and fluid inclusion assemblage in beryl from pegmatite in the Orlovka amazonite granite, East Transbaikalia, Russia: implications for pegmatite-forming melt systems. Petrology 96 (3–4), 129–140.
Thomas, R., Davidson, P., Beurlen, H., 2011a. Tantalite–(Mn) from the Borborema Pegmatite Province, northeastern Brazil: conditions of formation and melt- and fluid-inclusion constraints on experimental studies. Mineral. Deposita 46 (7), 749–759.
Thomas, R., Webster, J.D., Davidson, P., 2011b. Be-daughter minerals in fluid and melt inclusions: Implications for the enrichment of Be in granite–pegmatite systems. Contrib. Mineral. Petrol. 161 (3), 483–495.
Trueman, D.L., Černý, P., 1982. Exploration for rare-element granitic pegmatites. Short Course in Granitic Pegmatites in Science and Industry, pp. 463–493.
Trumbull, R.B., 1995. A fluid inclusion study of the Sinceni rare-element pegmatites of Swaziland. Petrology 55 (1), 85–102.
Wang, D., Zou, T., Xu, Z., Yu, J., Fu, X., 2004. Advance in the study of using pegmatite deposits as the tracer of orogenic process. Adv. Earth Science 19, 614–620.
Wang, H., Li, P., Dong, R., Zhou, K., 2017. Discovery of the Bailongshan superlarge lithium–rubidium deposit in Karakorum, Hetian, Xinjiang, and its prospecting implication. Geotecton. Metallog. 41, 1053–1062.
Wen, Z., Mao, J., 2002. Progress in supercritical fluid technology and its implication for metallogenesis. Geol. Rev. 48, 106–112.
Xiao, J., Fan, C., 2001. Progress in research of supercritical fluid technology. Progr. Chem. 13 (2), 94–101.
Xu, Z., Wang, R., Zhao, Z., Fu, X., 2018. On the structural backgrounds of the large-scale "hard-rock type" lithium ore belts in China. Acta Geol. Sin. 92, 1091–1106.
Yan, Q., Qiu, W., Wang, H., Wang, M., Wei, X., Li, P., Zhang, R., Li, C., Liu, J., 2016. Age of the Dahongliutan rare metal pegmatite deposit, West Kunlun, Xinjiang (NW China): Constraints from LA–ICP–MS U–Pb dating of columbite-(Fe) and cassiterite. Ore Geol. Rev. 100, 561–573.
Zhang, D., 1997. Some new advances in ore-forming fluid geochemistry on boiling and mixing of fluids during the processes of hydrothermal deposits. Adv. Earth Science 12, 546–552.
Zhou, B., Sun, Y., Kong, D., 2011. Geological features and prospecting potential of rare metallic deposits in the Dahongliutan region, Xinjiang. Acta Geol. Sichuan 31 (3), 288–292.
Zhu, J., Wu, C., Liu, C., Li, F., Xiao, H., Zhou, D., 2000. Magmatic–hydrothermal evolution and genesis of Koktokay No. 3 rare metal pegmatite dyke, Altai, China. Geol. J. China Univ. 6, 40–52.